Influence of frost on the bond between steel and concrete

Influence of frost on the bond between steel and concrete

K. Zandi Hanjari
CBI Swedish Cement and Concrete Research Institute, Borås, Sweden
Chalmers University of Technology, Gothenburg, Sweden

Peter Utgenannt
CBI Swedish Cement and Concrete Research Institute, Borås, Sweden

K. Lundgren & M. Plos
Chalmers University of Technology, Gothenburg, Sweden

ABSTRACT: In an experimental investigation, the effect of frost on bond properties between concrete and reinforcement was studied using pull-out tests. Compression tests and elastic modulus tests were carried out to study the concrete behavior in compression, and the tensile behavior of frost-damage concrete was investigated by splitting tensile tests. The test results showed significant change in material and bond properties of frost-damaged concrete compared to reference concrete. A methodology was introduced to predict the mechanical behavior of reinforced concrete structures with an observed amount of frost damage at a given time. The methodology was applied to concrete beams affected by internal frost damage, using non-linear finite element analyses. A comparison of the results indicated that, to a rather large extent, the effect on failure load caused by internal frost damage can be predicted by using the proposed methodology.

1 INSTRUCTION

One of the severe types of deterioration in concrete structures is associated with the volume expansion of concrete caused by freezing and thawing of concrete. Frost damage in concrete is caused by (a) the differing thermal expansion of ice and concrete and (b) by the volume expansion of freezing water in the concrete pore system; see Chatterji (1999). The former mechanism is involved when the structure is subjected to cold climates in the presence of saline water. The stress arises from the difference in thermal expansion of ice and concrete, which leaves the ice in tension as the temperature drops. Therefore, a crack in brine ice penetrates into the substrate and causes the superficial damage known as surface scaling; see Valenza & Scherer (2006). This damage usually results in spalling of the concrete surface, while the remaining concrete is mostly unaffected, see Wiberg (1993). The latter mechanism is involved when the volume expansion of the freezing water, restrained by the surrounding concrete, cannot be accommodated in the pore system. Thereby, tensile stresses are initiated and micro and macro cracks are introduced into the concrete body, which leads to the type of severe damage known as internal frost damage. This mechanism not only affects the compressive strength, tensile strength, elastic modulus and fracture energy, but also influences the bond strength between the reinforcement and surrounding concrete in damaged regions, sees Powers (1945), Shih et al. (1988) and Fagerlund et al. (2001).

Several research articles have been primarily concerned with the causes and mechanisms of frost deterioration, see Powers (1945), Beaudoin et al. (1974) and Utgenannt (2004). However, very little attention has been given to the effect of frost damage on the bond properties of concrete. Shih et al. showed that cyclic temperature changes have a decisive influence on the maximum bond resistance of concrete subjected to monotonic and reversed cyclic loading. Experimental observation proved that the bond stress-slip relation before maximum bond stress is similar for damaged and undamaged concrete; see Petersen et al. (2007). However, the bond capacity and slip at the maximum bond strength change significantly with frost damage; see Fagerlund et al. (2001).

The present paper deals with the effect of internal frost damage on the bond properties of concrete. Pull-out tests were carried out and the results were used to device a methodology to analyze the mechanical behavior and to determine the remaining load-carrying capacity of reinforced concrete structures affected by frost damage. Finally, the methodology was applied to concrete beams affected by internal frost damage, using non-linear finite element analyses.

2 EXPERIMENT

2.1 *Test program*

The experiments presented here were carried out to investigate the effect of frost damage on the material and bond properties of concrete. Therefore, the level of frost damage was quantified by the relative dynamic modulus of elasticity, calculated from ultrasonic measurements made on all specimens, and by the compressive strength of concrete. The change in microstructure of the concrete was visually observed by microscopic imaging; the distribution of cracks was investigated using image analysis of thin sections. The behavior of frost-damaged concrete was evaluated in compression, by compression tests and elastic modulus tests, and in tension, by splitting tensile and wedge splitting tests. Crack propagation in wedge splitting tests was monitored by measurements of the strain field using an optical system. The wedge splitting test made it possible to obtain the stress-crack opening, σ-ω, and fracture energy of concrete by inverse analysis. Pull-out tests were made to evaluate the effect of frost damage on the bond between the reinforcement and the concrete. Here only a summary of the pull-out test is given below; details concerning other tests are available in Zandi Hanjari (2008) and Zandi Hanjari et al. (2011).

Several tests were made on a reference specimen and frost-damaged concrete. Since the level of frost damage depends on the shape and size of the specimen, concrete cylinders of 250 × 100 mm were cast for all of the tests; these were cut by 25 mm at each end at the time of testing, see Figure 1. Due to limited space in the freezing chamber, the size of the specimens was chosen to be smaller than the standard size, cylinder 300 × 150 mm. The specimens were exposed to demineralised water to make sure that surface scaling was minimized. Twenty-four hour freeze-thaw cycles at temperatures from +20 °C to -20 °C, based on RILEM TC 176-IDC, were applied. The tests were made on:

(a) 28-day cured concrete called reference;

(b) 28-day cured concrete stored in a freezing chamber as long as needed to cause a reduction of 25% in compressive strength, damage level I; and

(c) 28-day cured concrete stored in a freezing chamber as long as needed to cause a reduction of 50% in compressive strength, damage level II.

2.2 *Pull-out test set-up*

The pull-out tests were designed to investigate the effect of frost on the local bond-slip relationship under well confined conditions. Therefore, the specimens should have been large enough not only to prevent splitting cracks but also to provide sufficient confinement to get pull-out failure. Since the pull-out specimens were 200 × 100 mm, the rebar diameter was chosen so that pull-out failure would take place. Nine molds were arranged for pull-out tests by placing a rebar of Ø6 mm on the axis through the center of the cylinder. The geometry of the specimens is given in Figure 1. The rebar was fixed by a plastic cone on the bottom plate and a wooden cross on the top of the mold. The embedment length was three times the bar diameter, i.e. 18 mm, which included 4 ribs; see Figure 1. The number of ribs and their location along the embedment length were kept constant in all specimens. The bars were debonded outside the embedment length by a plastic tube and the transition between the naked bar and the plastic tube was plunged with wax. This ensures a well-defined embedment length. The bar, plastic tube and plastic cone for fixing the rebar in the molds were assembled as shown in Figure 1.

The tests were conducted in a displacement controlled regime, which means that the active end-slip increased at a constant rate. The displacement rate initially was 0.1 mm/min and increased to 1.5 mm/min when the active end-slip reached 10 mm. The prescribed displacement was applied in the direction opposite to that of the casting.

The active and passive end-slips of the reinforcement bar were measured by five linear LVDTs. Four LVDTs were positioned at the passive end-slip, and one at the active end-slip. All data were stored in a computer and the active end-slip was plotted continuously versus the load by a xy-plotter.

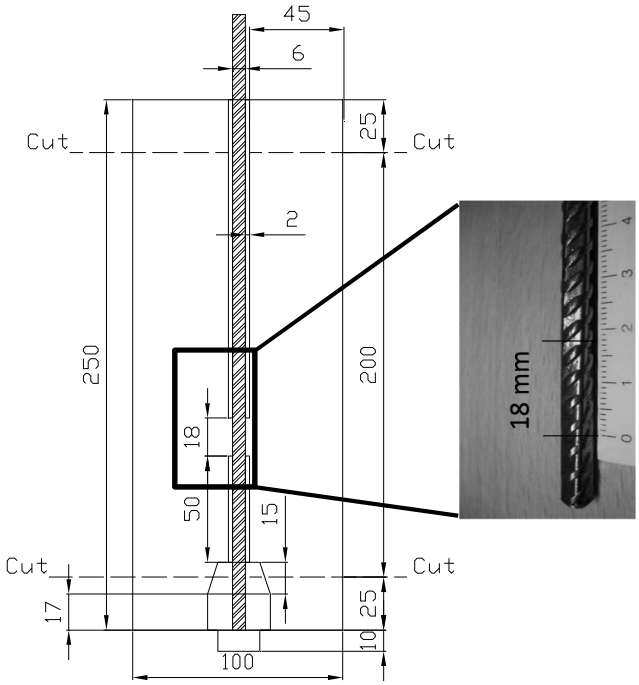

Figure 1. Geometry of the pull-out specimen rebar

2.3 *Material properties*

The concrete used in this investigation was of grade C35/45, with a water cement ratio (w/c) of 0.57. Through the casting, concrete was poured into the molds and compacted in two steps, 20 seconds vi-

bration using a vibrating table for each step. All the specimens were demolded after 24±2 hours and submerged in tap water at 20±2 ˚C for 7 days. Then the specimens were stored in a climate chamber, with a temperature of 20±2 ˚C and a relative humidity of 65±5 %, for 17 days. The specimens were presaturated by storing in tap water at 20±2 ˚C for 3 days. Subsequently, the reference specimens were tested and the others were stored in the freezing chamber to reach the desired level of frost damage, 25 and 50% reduction in compressive strength, damage level I and II, respectively. The specimens used for testing at the damage level I and II also were presaturated for 3 days prior to testing. The material properties of concrete are given in Table 1.

Table 1. Compressive and splitting tensile strength.

Concrete	Compression		Tensile	
	Strength (MPa)	Cov (%)	Strength (MPa)	Cov (%)
Reference	40.58	0.94	3.81	10.06
Damage level I	29.72	10.02	2.71	5.66
Damage level II	20.44	5.31	1.44	8.33

2.4 *Frost-damage quantification*

In a pilot study, some tests were conducted on a limited number of concrete cylinders to study how the level of frost damage can be quantified by different methods, as well as how early the frost damage affects concrete compressive strength. The specimens were cast from the same concrete composition as the main study, and they were subjected to freeze-thaw cycles for two weeks. The pilot study included ultrasonic transit time measurements and fundamental transverse frequency tests, carried out every day, as well as compressive tests, made every few days. The results showed that ultrasonic tests were more sensitive to frost damage; the measurements were more stable than fundamental transverse frequency tests. Therefore, it was decided to use ultrasonic tests to monitor the level of frost damage in the main study.

In the main study, the level of damage was monitored by ultrasonic measurements of all specimens, after every three freeze-thaw cycles, and by compressive strength tests, when the ultrasonic measurements showed a significant change of transmission time. Once the desired reduction in compressive strength was reached, the specimens were chosen that had approximately the same reduction in the ultrasonic measurements as the one tested in compression. These specimens were removed from the freezing chamber and prepared for testing.

2.5 *Freeze-thaw exposure*

After 28-day curing, the specimens were placed in a cylindrical water container, 260 × 110 mm, and exposed to freeze-thaw cycles in a temperature controlled chamber. This means that the specimens were covered with 5 mm of demineralized water on all surfaces while they were subjected to repeated freezing and thawing. During the test, the temperature in the freezing chamber for all specimens followed the regime specified in RILEM TC 176-IDC, i.e. Twenty-four hour freeze-thaw cycles at temperatures from +20 °C to -20 °C.

2.6 *Test results*

The bond stress-slip response was deduced by converting the measured forces from the pull-out tests into bond stresses:

$$\tau_b = \frac{F}{\pi \cdot \phi \cdot l_e} \tag{1}$$

where F is the force, measured in the pull-out test, $\emptyset$ is the nominal bar diameter, and l_e is the embedment length. More details of measurements, such as the actual embedment length and the maximum measured tensile force for each of the pull-out specimens have been reported in Zandi Hanjari (2008). The bond-slip response for different levels of frost damage characterized by the compressive strength is shown in Figure 2.

All tests resulted in pull-out failure at steel stresses below the yield strength, and the failure mode was characterized by shear sliding along the gross perimeter of the rebar. The bond capacity is reduced by 14 % and 50 % for damage levels I and II, respectively. The stiffness of the ascending branch of the bond-slip response decreased with frost damage. Moreover, the slip at the maximum force increased with frost damage (0.39, 0.48 and 0.60 mm for the reference, and damage levels I and II, respectively). The bond stress remained more or less constant over a limited range before dropping.

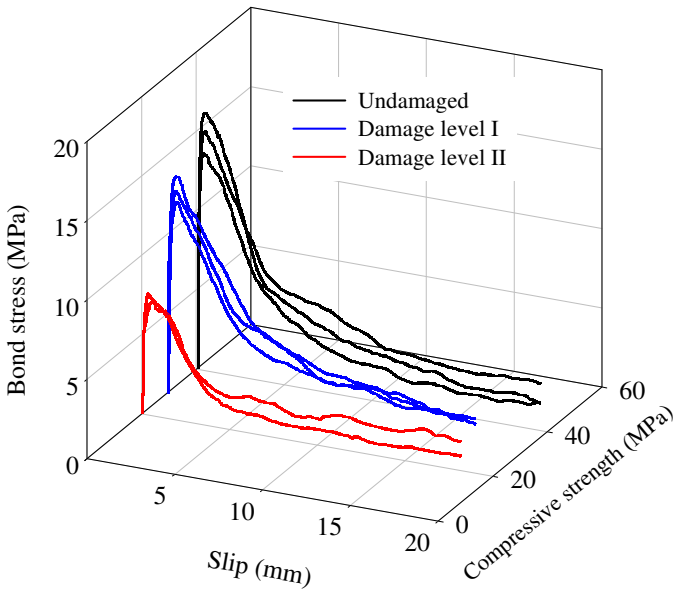

Figure 2. Bond-slip response.

3 STRUCTURAL ANALYSIS

3.1 *Methodology*

A methodology to analyze the mechanical behavior and to determine the remaining load-carrying capacity of reinforced concrete structures affected by frost damage was presented in Zandi Hanjari et al. (2011). The methodology is based on the premise that the effect of internal frost damage can be modeled as changes in material and bond properties. Moreover, the effect of surface scaling can be taken into account as a change in geometry, such as a reduction in concrete cross-section when surface scaling leads to cover spalling while the remaining concrete is assumed to be unaffected, Wiberg (1993). The methodology is restricted to the prediction of the mechanical behavior of a structure with an observed amount of damage at a given time; hence, the formation of the damage over time is not included.

In the assessment of the damaged structures, the compressive strength and the dynamic modulus of elasticity, as indicators of damage, must be measured in each individual case. The compressive strength can be evaluated by compression tests on a few drilled cores, supplemented with non-destructive tests to determine the extent of the damaged region. The dynamic modulus of elasticity can be evaluated using either ultrasonic transit time measurement or fundamental transverse frequency test. It is believed that there is a strong correlation between the level of frost damage, in term of the reduction in compressive strength, and the dynamic modulus of elasticity, Petersen et al. (2007). Such a correlation has been suggested in Zandi Hanjari et al. (2011) using the available test data in the literature. Thereafter, the effect of frost damage on material properties, such as the stress-strain response in compression, the stress-crack opening relation in tension and the bond-slip behavior, is estimated using the damage indicators. Finally, the behavior of the damaged structure can be studied in the finite element (FE) analysis. Within this context, suggestions were given on how the effect of frost can be taken into account as changes in the effective material and bond properties in Zandi Hanjari et al. (2011). Here the later part, effect of frost on bond properties, is further discussed.

3.2 *Bond behavior*

Available experimental studies concerning the effect of frost damage on the bond between the reinforcement and concrete lead to the following three conclusions:

1) In spite of a large scatter, the tests show an obvious influence of frost on the bond strength. Fagerlund *et al.* (1994) suggested lower and upper bound values for the reduction of the bond strength equal to 30 and 70%. The test results presented in Section 2 shows 14 and 50% bond deterioration for frost damage levels equivalent to 25 and 50% reduction in compressive strength. A linear decrease of the bond strength with the increase of damage was suggested by other researchers; see Petersen *et al.* (2007) and Ji *et al.* (2008).
2) For a low level of damage, when the effect of frost is limited to the concrete cover, a small decrease of the slip at the maximum bond stress is observed; see Petersen *et al.* (2007). For a large damage, when the effect of frost is extended to the interface between the concrete and the reinforcement, the bond capacity suddenly decreases and the slip slowly increases; see Shih *et al.* (1988), Petersen *et al.* (2007) and Zandi Hanjari *et al.* (2009).
3) The residual bond strength, represented by a constant stress after the descending branch of the bond stress-slip relationship, decreases with increased damage level; see Zandi Hanjari *et al.* (2009).

The bond stress-slip relation proposed by CEB-FIB Model Code 90 (1993) is here modified to incorporate frost effects. In regions where the concrete cover has totally spalled off due to surface scaling, the bond strength is assumed to be zero. In other areas where the cover still remains (but may be cracked), the bond-slip properties are estimated based on the following approximations:

1) The relation between bond strength, τ_b, and slip, s, given in CEB-FIB Model Code 90 (1993) are adopted for the undamaged concrete. To account for intermediate cases in between the extreme cases “confined” (i.e. ductile pull-out failure) and “unconfined” (i.e. brittle failure due to cover cracking induced by the radial tensile stress), the following interpolation formula was proposed by Lundgren et al. (2012):

$$\tau_b = k_{\text{int}} \cdot \tau_{b,confined} + (1 - k_{\text{int}}) \cdot \tau_{b,unconfined} \tag{2}$$

The interpolation factor is determined by

$$k_{\text{int}} = \max \begin{cases} k_{c/\phi} \\ k_{Asw} \end{cases} \tag{3}$$

where $k_{c/\phi}$ is a factor that depends on the ratio of cover to bar diameter, c/ϕ; k_{Asw} is a factor that depends on the amount of effective shear reinforcement, A_{sw}/s_w; and s_w is the shear reinforcement spacing. Factors $k_{c/\phi}$ and k_{Asw} are chosen according to Figure 3.

2) The variation of the maximum bond stress in relation with the frost damage quantified

with the relative dynamic modulus of elasticity was formulated by Petersen *et al.* (2007):

$$\tau_{\max}{}^{d} = \left(0.17 + 0.007 \cdot E_{D,rel}{}^{d}\right) \cdot \tau_{\max} \quad (4)$$

where $\tau_{\max}{}^{d}$ and $\tau_{\max}$ are the bond strength for damaged and undamaged concrete, respectively, and $E_{D,rel}{}^{d}$ is the relative dynamic modulus of elasticity for the damaged concrete.

3) The residual bond strength is reduced proportionally to the reduction in the bond capacity; see Zandi Hanjari *et al.* (2009).

$$\tau_{f}{}^{d} = \left(\frac{\tau_{\max}{}^{d}}{\tau_{\max}}\right) \cdot \tau_{f} \quad (5)$$

where $\tau_{f}{}^{d}$ and τ_{f} are the residual bond strength for damaged and undamaged concrete, respectively.

The analytical bond-slip relation for the damaged concrete is compared with the test results presented earlier in Figure 4.

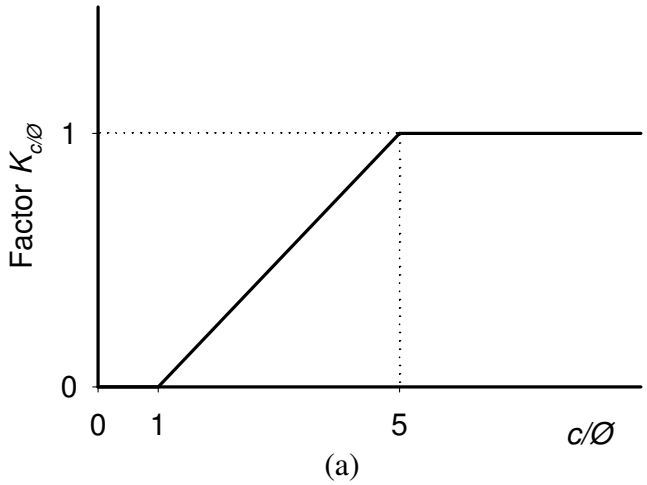

(a)

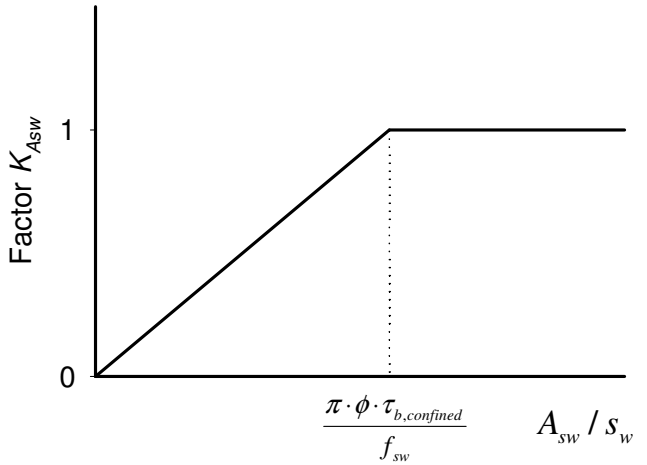

(b)

Figure 3. Interpolation factors from Lundgren *et al.* (2012).

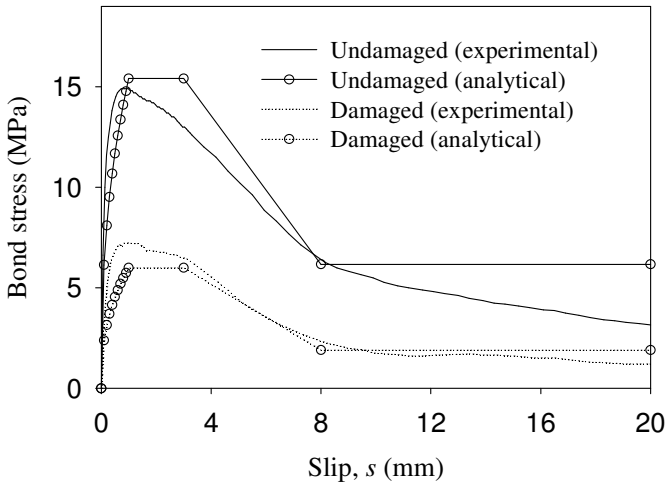

Figure 4. Bond-slip relation for "Good" bond condition; the level of frost-damage corresponds to 50% reduction in compressive strength.

4 APPLICATION OF THE METHODOLOGY

4.1 *Frost-damaged beam tests*

In an experimental program, Hassanzadeh & Fagerlund (2006) have studied the effect of frost damage on the load-carrying capacity of beams. Several beam tests were carried out including two geometries with varied reinforcement content and stirrups; see Table 2 and Figure 5. The reference beams were exposed to a laboratory climate. The other beams were vacuum treated to a residual pressure of 2 mmHg followed by submerging in water. Thereafter, they were subjected to two complete freeze-thaw cycles with a constant temperature at -21±1ºC inside a climate chamber. The compressive strength, splitting tensile strength and fracture energy of concrete have been measured. The splitting tensile strength of the concrete exposed to freezing has been determined for 80 × 80 mm cores drilled from concrete blocks of 1 × 0.4 × 0.2 m stored under the same conditions as the damaged beams. The specimens exposed to freezing showed typical internal frost damage with no sign of surface scaling.

Table 2. Beam types (Hassanzadeh and Fagerlund 2006).

Type	*l* *[m]*	*h* × *b* *[mm]*	*Tensile reinforcement*	*Stirrup*	*Beam names*	
					Reference	*Damaged*
5	4.4	500 × 200	4Ø20	8Ø8	R5	D5
6	3.0	300 × 200	3Ø20	8Ø8	R6	D6

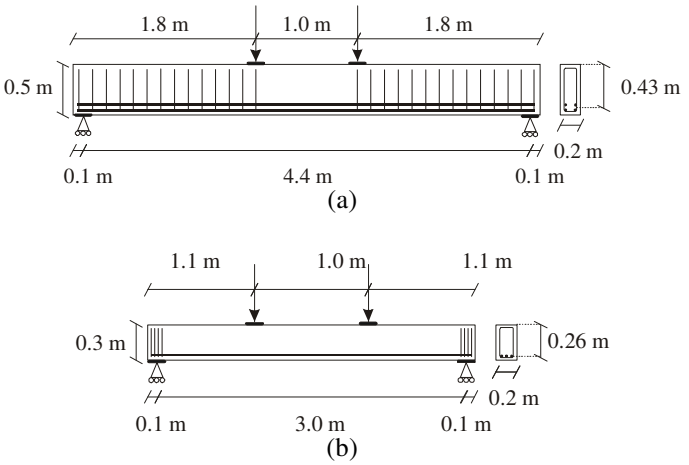

Figure 5. Examples of the beam: (a) type 5 and (b) type 6 (Hassanzadeh & Fagerlund, 2006).

4.2 *FE model and numerical procedure*

The load-carrying capacity of the reference and frost-damaged beams, tested by Hassanzadeh & Fagerlund (2006), was calculated with 2D finite element analysis according to the proposed methodology. The beams were modeled using plane stress elements and the interaction between the longitudinal reinforcement and the concrete was modeled with a bond-slip mechanism; however, the stirrups were embedded in the plane stress concrete elements by assuming full interaction.

An incremental static analysis was made using an explicitly specified load step size and a Newton-Raphson iterative scheme to solve the non-linear equilibrium equations. In a phased analysis, the self-weight load was first applied. Thereafter, the beam was subjected to the external load as a prescribed displacement at the loading point.

4.3 *Modeling of concrete-reinforcement interaction*

The longitudinal reinforcement was modeled by two-node truss elements. Interaction between the reinforcement and the concrete was modeled with a bond-slip relation. Interface elements, describing the bond-slip behavior in terms of a relation between the tractions and the relative displacements, were used across the reinforcement and the concrete interface. The analytical bond-slip relation for confined concrete under "Good" bond conditions given in the CEB-FIP Model Code (1990) was assumed for the reference beams. The same relation was adapted according to the proposed modifications and used in the analysis of the damaged beams. The stirrups were embedded in the concrete elements, corresponding to a perfect bond between the stirrups and concrete. The embedded stirrups add stiffness to the concrete elements; their strain is calculated from the displacement field of the plane stress elements (DIANA 2009).

5 RESULTS AND DISCUSSION

With respect to the design rules for reinforced concrete beams at the ultimate limit state, the failure mode of an undamaged beam depends on the reinforcement ratio, in such a way that a lightly reinforced beam is expected to fail in bending due to yielding of reinforcement, while a heavily reinforced beam is excepted to fail in bending due to concrete crushing. A moderately reinforced beam may fail in either of the modes. A flexural member is also subjected to shear stresses which may lead to diagonal cracks. Unless a properly detailed cross-section and appropriate amount of transverse and longitudinal reinforcements are provided, diagonal cracks may results in shear failure. Other failure modes may also govern the behavior of a beam; however, the beams in the experimental program of Hassanzadeh & Fagerlund (2006) were designed to fail in one of the described modes.

The results from the numerical analyses and experiments are presented and compared. The load versus midspan deflection of the beams from the experiments and the numerical analyses are presented in Figures 6 and 7. The crack distributions in terms of principal tensile strains from the analyses are shown in Figures 8 and 9.

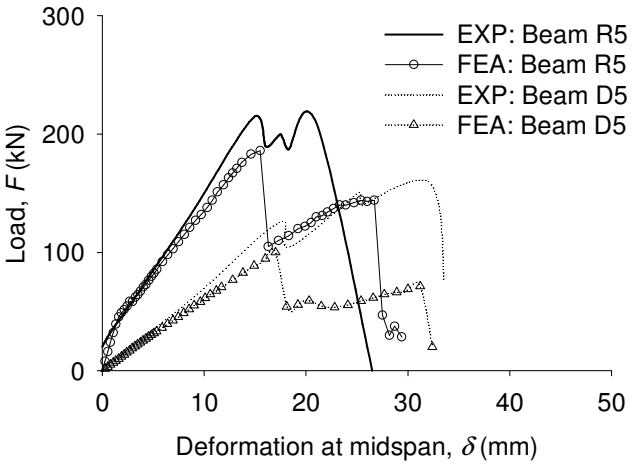

Figure 6. Load-deformation for beams type 5.

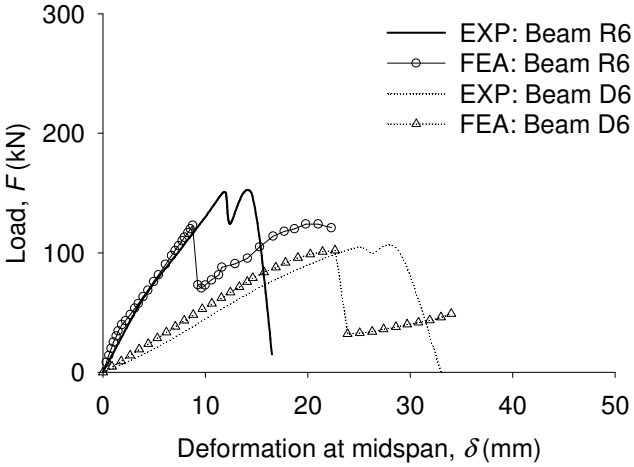

Figure 7. Load-deformation for beams type 6.

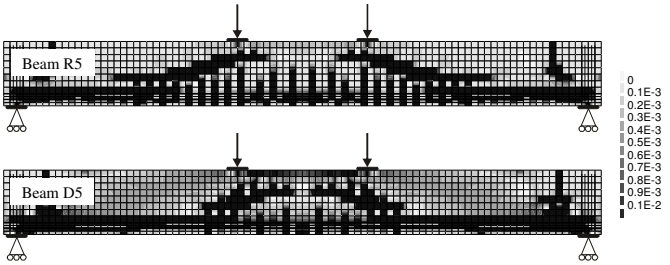

Figure 8. Crack pattern in terms of the maximum tensile strains from numerical analyses of beams (a) type 1, (b) type 3 and (c) type 5.

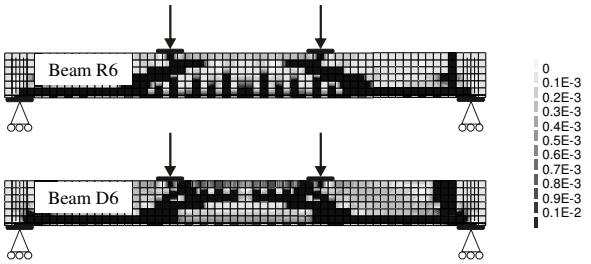

Figure 9. Crack pattern in terms of the maximum tensile strains from numerical analyses of beams (a) type 2, (b) type 4 and (c) type 6.

The load versus the deformation of the reference beam R5, which has the larger cross-section, is plotted in Figure 6. Diagonal shear cracking limited the capacity of the beam in the test at a load of approximately 220 kN; this was estimated to be about 200 kN according to the provisions given in EuroCode 2. The numerical analysis estimated a failure load of approximately 190 kN and showed that inclined shear cracking governed the failure of the beam. The evolution of cracks in the analysis explains the two peak loads at about 190 and 140 kN observed in the analysis. In the analysis, Figure 8, a few bending cracks formed for a rather small load levels; this caused the change in the initial stiffness. For a larger load, shear cracks appeared and reached the tensile reinforcement in the middle of the shear span; this governed the failure of the beam and formed the first peak in the load-deformation curve. Thereafter, longitudinal cracks propagated along the reinforcement towards the end of the beam. These cracks stopped at the support regions where four closely spaced stirrups were placed. Finally, the formation of the vertical cracks next to the support resulted in an anchorage failure; this corresponds to the second peak in the load.

A rather large influence of frost was seen in the capacity of this beam, Figure 6. The beam D5 failed in shear, similar to the reference beam, at a load level of 125 kN. This was estimated to be approximately 150 kN according to EuroCode 2 using the damaged material properties. The analysis also showed a shear failure at a load of approximately 110 kN followed by an anchorage failure in the support region, Figure 8. The evolutions of diagonal and longitudinal cracks in the analysis were similar to that of the reference beam. The crack pattern from the numerical analysis showed that the diagonal cracks in the damaged beam formed with a greater angle to the longitudinal axis compared to the diagonal cracks in the reference beam. This is mainly because of the effect of frost on the compressive strength of concrete. As the compressive strength decreases, the shear stress required to cause cracking decreases and the inclination of the cracks to the longitudinal axis increases.

Beam type 6 had the same amount of shear reinforcement as the beam type 5 but with smaller cross-section. Therefore, larger effect of frost was expected on the capacity of beam type 6 as it was more damaged. For both the reference and the damaged beams, shear cracking limited the load capacity in the experiments and the analyses, Figures 7 and 9. Numerical analysis estimated the capacity of the damaged beam quite well.

The results from numerical analysis kept on the safe side. The load capacity and the deformation at the failure loads were slightly underestimated. This can be explained by two aspects of the analysis: a) the tension softening of concrete and b) the stiffness of longitudinal reinforcement in transverse direction. When concrete cracks, tensile stresses are transferred due to tension softening. In reinforced concrete, stresses are also transmitted across the crack by the bond action between the reinforcement and the concrete. In a situation where the crack is subjected to shear loading, additional stresses are transferred due to friction. Therefore, if tension softening of concrete is estimated when only fracture energy of concrete is taken into account, the results will keep on the safe side, Broo *et al.* (2008), as it was in the analyses presented here. The second explanation concerns with the modeling of longitudinal reinforcement. When diagonal cracks form, the ability of concrete to transmit tensile stresses is severely reduced unless appropriate reinforcement is present. In reality, the reinforcement has stiffness parallel and perpendicular to the bar axis. However, the tensile reinforcement, modeled with truss elements in the FE analysis, had stiffness only along the bar axis. This contributes to underestimation of the results in the post-peak behavior.

6 CONCLUSIONS

In an experimental study, the effect of frost damage on the material and bond properties of concrete was investigated. The level of frost damage was quantified using ultrasonic measurements together with the compressive strength of concrete. Compression tests and elastic modulus tests were conducted to study the concrete behavior in compression, and the tensile behavior of frost-damage concrete was investigated

by splitting tensile tests and wedge splitting tests. Finally, pull-out tests were performed to evaluate the effect of frost damage on the bond between the reinforcement and the concrete.

A methodology to analyze the mechanical behavior of reinforced concrete structures affected by frost damage was introduced. It was proposed that the effects of internal frost damage and surface scaling can be modeled as changes in the material and bond properties as well as the cross-section of the damaged concrete member. Then, the proposed methodology was tested on concrete beams affected by internal frost damage. The results of the analyses were compared with the available beam tests, Hassanzadeh & Fagerlund (2006). Based on this study the following conclusions are drawn.

1) The test results showed significant change in the material and bond properties of frost-damaged concrete when compared with reference concrete.
2) The pull-out test results showed a significant change in the bond properties of frost-damage concrete compared to reference concrete, i.e. the slip at the maximum bond stress increased with frost damage. The first level of damage, defined as 25 % reduction in compressive strength of concrete, corresponded to 14 % reductions in bond strength. For the second level of damage, defined as 50 % reduction in the compressive strength of concrete, bond strength was decreased 50 %.
3) The change in material and bond properties due to the effect of frost may lead to a change in the load-capacity and more brittle behavior of a structure at failure. A comparison of the results with available experimental data indicated that, to a rather large extent, the effect on failure load caused by internal frost damage can be predicted by using the proposed methodology.

7 REFERENCES

Shih, T. S., Lee, G. C. and Chang, K. C. 1988. Effect of freezing cycles on bond strength of concrete. *Journal of Structural Engineering,* Vol. 114, No. 3, pp. 717–726.

Petersen, L., Lohaus, L. and Polak, M. A. 2007. Influence of freezing-and-thawing damage on behavior of reinforced concrete elements. *ACI Materials Journal,* Vol. 104, No. 4, pp. 369–378.

Fagerlund, G., Somerville, G. and Jeppson, J. 2001. *Manual for Assessing Concrete Structures Affected by Frost*, EC Innovation Project IN30902I, CONTECVET: A validated user's manual for assessing the residual service life of concrete structures, Division of Building Materials, Lund Institute of Technology, Lund, Sweden.

Chatterji, S. 1999. Aspects of the freezing process in a porous material-water system: Part 1. Freezing and the properties of water and ice. *Cement and Concrete Research,* Vol. 29, No. 4, pp. 627–630.

Valenza, J. J. and Scherer, G. W. 2006. Mechanism for salt scaling. *Journal of the American Ceramic Society,* Vol. 89, No. 4, pp. 1161–1179.

Wiberg, U. 1993. *Material Characterization and Defect Detection in Concrete by Quantitative Ultrasonics*, Doctoral thesis, Institutionen för Byggkonstruktion, Kungl Tekniska Högskolan, Stockholm, 1993, 152 pp.

Powers, T. C. 1945. A working hypothesis for further studies of frost resistance of concrete. *Journal of the American Concrete Institute,* Vol. 16, No. 4, pp. 245–271.

Utgenannt, P. 2004. The Influence of Ageing on the Salt-frost Resistance of Concrete, Doctoral thesis, Division of Building Materials, Lund Institute of Technology, Lund, Sweden.

Beaudoin, J. J. and MacInnis, C. 1974. The mechanism of frost damage in hardened cement paste. *Cement and Concrete Research,* Vol. 4, No. 2, pp. 139–147.

Zandi Hanjari, K. 2008. Material and Bond Properties of Frost-Damaged Concrete. Department of Civil and Environmental Engineering, Chalmers University of Technology, Report nr 08:10.

Zandi Hanjari, K., Utgenannt, P. and Lundgren, K. 2011. Experimental study of the material and bond properties of frost-damaged concrete, Cement and Concrete Research, Vol 41, No 3, pp 244–254.

Tang, L. and Petersson, P. E. 2004. Slab test: Freeze/thaw resistance of concrete – Internal deterioration. *Materials and Structures,* Vol. 37, No. 274, pp. 754–759.

Fagerlund, G., Janz, M. and Johannesson, B. 1994. *Effect of frost damage on the bond between reinforcement and concrete*, A contribution to the BRITE/EURAM project BREU-CT92-0591, The Residual Service Life of Concrete Structures, Division of Building Materials, Lund Institute of Technology, Lund, Sweden.

Ji, X., Song, Y. and Liu, Y. 2008. Effect of freeze-thaw cycles on bond strength between steel bars and concrete. *Journal Wuhan University of Technology, Materials Science Edition,* Vol. 23, No. 4, pp. 584–588.

Zandi Hanjari, K., Utgenannt, P. and Lundgren, K. 2009. Frost-damaged concrete: Part 2. Bond properties. *The 4th International Conference on Construction Materials: Performance, Innovations and Structural Implications*, 24–26 Aug., Nagoya, Japan, pp. 761–766.

CEB 1993. *CEB-FIP Model Code 1990,* Bulletin d'Information 213/214, Lausanne, Switzerland.

Lundgren, K., Kettil, P., Zandi Hanjari, K., Schlune, H. and San Roman, A. S. 2012. Analytical model for the bond-slip behaviour of corroded ribbed reinforcement, Structure and Infrastructure Engineering, Volume 8, Issue 2, pp 157-169.

Hassanzadeh, M. and Fagerlund, G. 2006. Residual strength of the frost-damaged reinforced concrete beams. *The Proceedings of the III European Conference on Computational Mechanics Solids, Structures and Coupled Problems in Engineering,* Lisbon, Portugal.

DIANA 2009. *DIANA Finite Element Analysis, User's Manual, release 9.3.* TNO Building and Construction Research, Delft, Netherlands.

Broo, H., Lundgren, K. and Plos, M., 2008. A guide to nonlinear finite element modelling of shear and torsion in concrete bridges. Report 2008:18, Civil and Environmental Engineering, Chalmers University of Technology, Göteborg, Sweden.